Supplementary Figures

Figure S1. The antibody against H3.3S31ph is specific to H3.3S31ph. Immunofluorescence analysis was performed using antibodies against H3.3S31ph (green) and centromeres (human CREST antiserum; red). To validate the specificity of the anti-H3.3S31ph antibody, a H3.3S31 blocking peptide was co-incubated onto the microscope slides. **(A-C)** In telomerase positive A549 cells, H3.3S31ph (green) localised at the pericentric satellite DNA repeats (A) When the antibody is co-incubated with 100 ng of the H3.3S31 peptide, H3.3S31ph staining at the pericentric DNA repeats was reduced to below detection (B). The pericentric staining of H3.3S31ph was not reduced when a smaller amount (40 ng) of the H3.3S31 peptide was added (C). **(D-F)** A high level of H3.3S31ph staining was detected on the chromosome arms in W138-VA13/2RA ALT cells (D). The staining of H3.3S31ph was not observed when 100 ng of the H3.3S31 peptide was added (E**).** A low level of H3.3S31ph staining was detected on the chromosome arms when 40 ng of H3.3S31 peptide was added (F). Representative images of 50 chromosome spreads are shown. Scale bar =5μm.

Figure S2. An aberrant H3.3S31ph distribution pattern in human ALT cancer cell lines. Immunofluorescence analysis was performed using antibodies against H3.3S31ph (green) and centromeres (human CREST antiserum; red). **(A-B)** In telomerase positive HT29 and HT1080 cells, H3.3S31ph is enriched at pericentric DNA repeats. No enrichment was observed on chromosome arms. **(C)** In ALT positive SKLU1 cells, H3.3S31ph was enriched at the pericentric DNA repeats. **(D-G)** In ALT-positive G292 (D), SUSM1 (E), Saos-2 (F) and KMST6 (G) cells, H3.3S31ph was found at extremely high levels at the pericentric DNA repeats and chromosome arms. Representative images of 50 chromosome spreads are shown. Scale bar =5μm.

Figure S3. Intensity of H3.3S31ph distribution on the chromosome arms in ALT cancer cell lines.

Immunofluorescence analysis with antibody against H3.3S31ph (green) was performed on non-ALT **(A)** A549 cells and **(B-C)** ALT positive GM847 cells. The staining of H3.3S31ph was categorized into three different subgroups based on the enrichment and intensity level on chromosome arms (arbitrary units of <1000 denotes only pericentric localization; whereas >1000 indicates the enrichment of H3.3S31ph on the chromosome arm). (D) In A549 cells, greater than 90% of the H3.3S31ph was found at the pericentric region and less than 10% of the population has slight spreading of the H3.3S31ph staining on chromosome arms. In contrast, 50% of the mitotic population in GM847 cells has moderate enrichment of H3.3S31ph on chromosome arms and more than 20% have intense H3.3S31ph staining on the chromosome arms. Scale bar =5μm.

Figure S4. Loss of ATRX expression correlates with an increase in H3.3S31ph staining on the mitotic chromosomes. (A) Cell lysates were prepared from human telomerase positive and ALT cell lines. ATRX protein expression levels were examined by Western blot analysis. ATRX protein expression was lost in all ALT cell lines, with the exception of SKLU1 and G292. **(B)** ATRX expression was depleted in A549 (telomerase positive) and SKLU1 (ALT) cells by transfection of specific siRNA oligonucleotides against ATRX for 48 h. **(C-F)** Immunofluorescence analysis was also performed on A549 and SKLU1 cells 48 h post-transfection. In A549 and SKLU1 transfected with scramble control siRNA oligonucleotides, H3.3S31ph was found at the pericentric DNA repeats (C, E). When ATRX was depleted, H3.3S31ph staining remained prominent at the pericentric DNA repeats and, there was an increase (~2 fold) in H3.3S31ph staining on the chromosome arms (D, F). Representative image from 50 chromosome spreads. Scale bar =5μm.

Figure S5. No association between H3.3 expression and altered H3.3S31ph dynamics in ALT cancer cells. (A) Cell lysates were prepared from asynchronous telomerase positive A549 and ALT cell lines. H3.3 protein levels were determined by Western blot analysis. No significant difference in H3.3 protein level was observed among the cell lines examined, when compared to telomerase positive cancer cells. **(B)** Cells were arrested at the G2 boundary by the addition of RO-3306 for 16 h prior to being released into mitosis. Mitotic cells were enriched by incubation of cells with Colcemid for 3 h. No significant difference in H3.3 protein levels was detected between the mitotic telomerase positive and ALT cell lines.

Figure S6. Human ALT cancer cell lines are burdened with severe genome instability. (A) Immunofluorescence analysis was performed using antibodies against H3.3S31ph (green) and centromeres (human CREST antiserum; red). High level of DNA breakage or chromosome fragmentation was found in GM847 ALT cells (indicated by arrowheads). H3.3S31ph enrichment was not restricted to pericentric DNA repeats but extended across the chromosome arms. **(B)** Immunofluorescence analysis was performed using antibodies against γH2AX (green) and centromeres (human CREST antiserum; red). W138-VA13/2RA ALT cells showed increased staining of γH2AX not only at telomeres, but also on fragmented DNA (arrowheads). Representative images of 50 chromosome spreads were shown. Scale bar = 10μm.

Figure S7. CHK1 inhibition resulted in a reduction in the phosphorylation of H3.3S31ph in ALT cancer cell lines. Human ALT cancer cell lines, SUSM1 (A-B) and KMST6 cells (C-D)

were arrested at G2 boundary using RO-3306. They were then released into mitosis either in the presence or absence of CHK1 inhibitor SB218078 (Chk1i) for 20 min. Immunofluorescence analysis indicated that both lines showed extremely high levels of H3.3S31ph (green) at the pericentric satellite DNA repeats and chromosome arms **(A, C)**. Treatment of cells with CHK1 inhibitor SB218078 (Chk1i) **(B, D)** resulted in a significant reduction in the level of H3.3S31ph. Centromeres were stained with a human CREST antibody (red). Representative images of 50 spreads are shown. Scale bar = 10μm.

Fig. S8. Depletion of CHK1 affects the cell-cycle distribution in ALT cancer cells. (A-B) (i) Cell lysates were collected from CHK1 depleted (Ai) telomerase positive A549 and (Bi) U2OS ALT cells. CHK1 protein levels were examined by Western blot analysis. (ii) RNA was collected from (Aii) A549 and (Bii) U2OS cells transfected with either Scramble control or CHK1 specific siRNA oligonucleotides. CHK1 expression levels were determined by quantitative realtime PCR. CHK1 expression was reduced to 20-30% 48 h post-transfection. (iii) Cell-cycle profiles of CHK1-depleted A549 and U2OS cells were assessed by FACS analysis. In A549 cells, an increase in the G1 cell population was observed 48 h post-transfection of CHK1 siRNA oligonucleotides. In U2OS cells, siRNA depletion of CHK1 protein led to an increase in S-phase cell population. In addition, a reduction in G2/M cell population was observed. Graphs represent an average ± standard error from three independent experiments. **(C)** Immunofluorescence analysis was performed to determine the level γH2AX in CHK1 depleted A549 and U2OS cells. Compared to the cell populations transfected with the Scramble control siRNA oligonucleotides (Ci, iii), a greater percentage of the cell population was found to show γH2AX (red) staining when transfected with CHK1-specific siRNA oligonucleotides (Cii, iv). Furthermore, γH2AX level is found to be extremely high in U2OS cell population depleted of CHK1. Scale = 10 μm.

Figure S9. CHK1 inhibition results in increased γH2AX in ALT cancer cell lines. Human telomerase positive A549 (A-B) and GM847 ALT cells (C-D) were arrested at G2 boundary using RO-3306. They were then released into mitosis either in the presence or absence of CHK1 inhibitor SB218078 (CHK1i). Immunofluorescence analysis of cells treated with CHK1 inhibitor SB218078 (CHK1i) resulted in a significant increase in γH2AX (red) staining in GM847 cells on the chromosome arms and at the telomeres, whereas CHK1 inhibition in A549 did not lead to a significant increase in γH2AX, **(B, D).** Centromeres were stained with a human CREST antibody (red). Representative images of 50 spreads are shown. Scale bar = 10μm.

Figure S10. Substitution of the Serine 31 with an Alanine residue alters the H3.3 S31ph staining pattern in ALT positive cancer cells. Cell lysates were prepared from HeLa and W138-VA13/2RA cells expressing either mycH3.3 (WT) or mutant mycH3.3S31A (S31A). These cells were harvested 96 h post-transfection. Cell lysates were also prepared from untransfected W138-VA13/2RA cells and a mouse embryonic stem (ES) cell line expressing mycH3.3, and they were used as negative and positive controls, respectively. Western blot analysis was performed with an antibody against the myc tag. Histone H3 was used as a loading control.

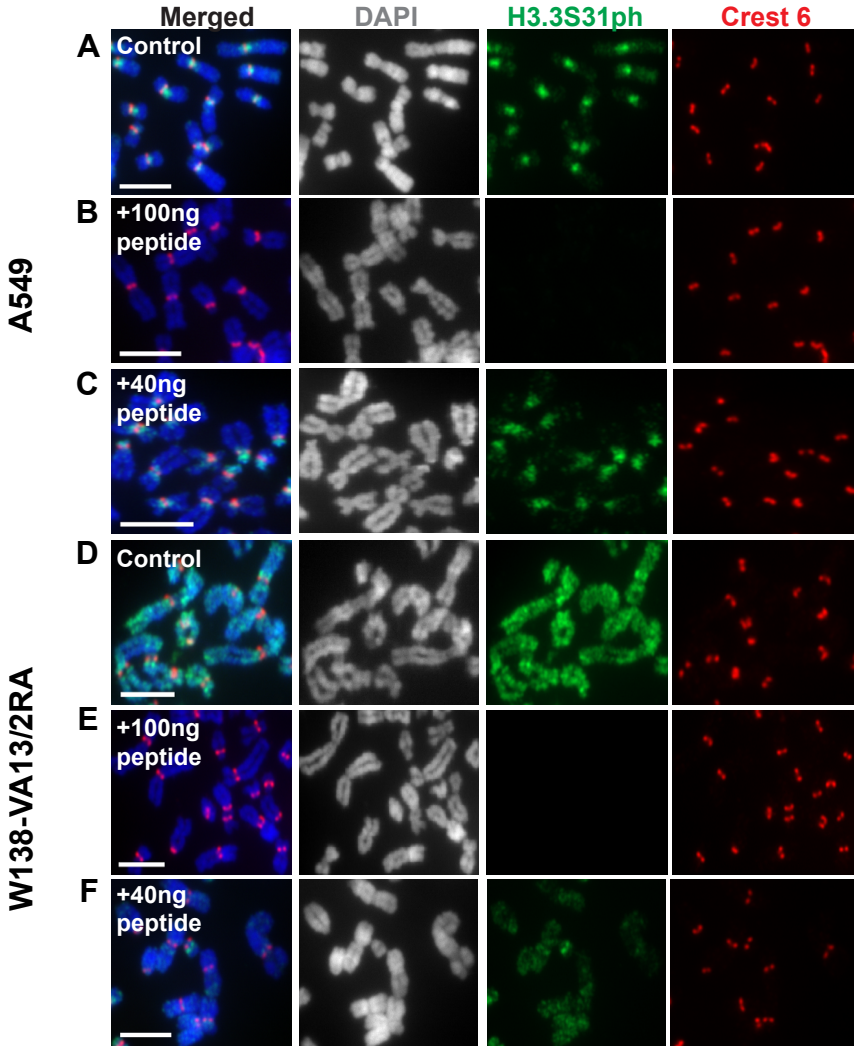
Merged
DAPI
H3.3S31ph
Crest 6
A
Control
B
+100ng
peptide
C
+40ng
peptide
D
Control
E
+100ng
peptide
F
+40ng
peptide
A549
W138-VA13/2RA

Figure S1

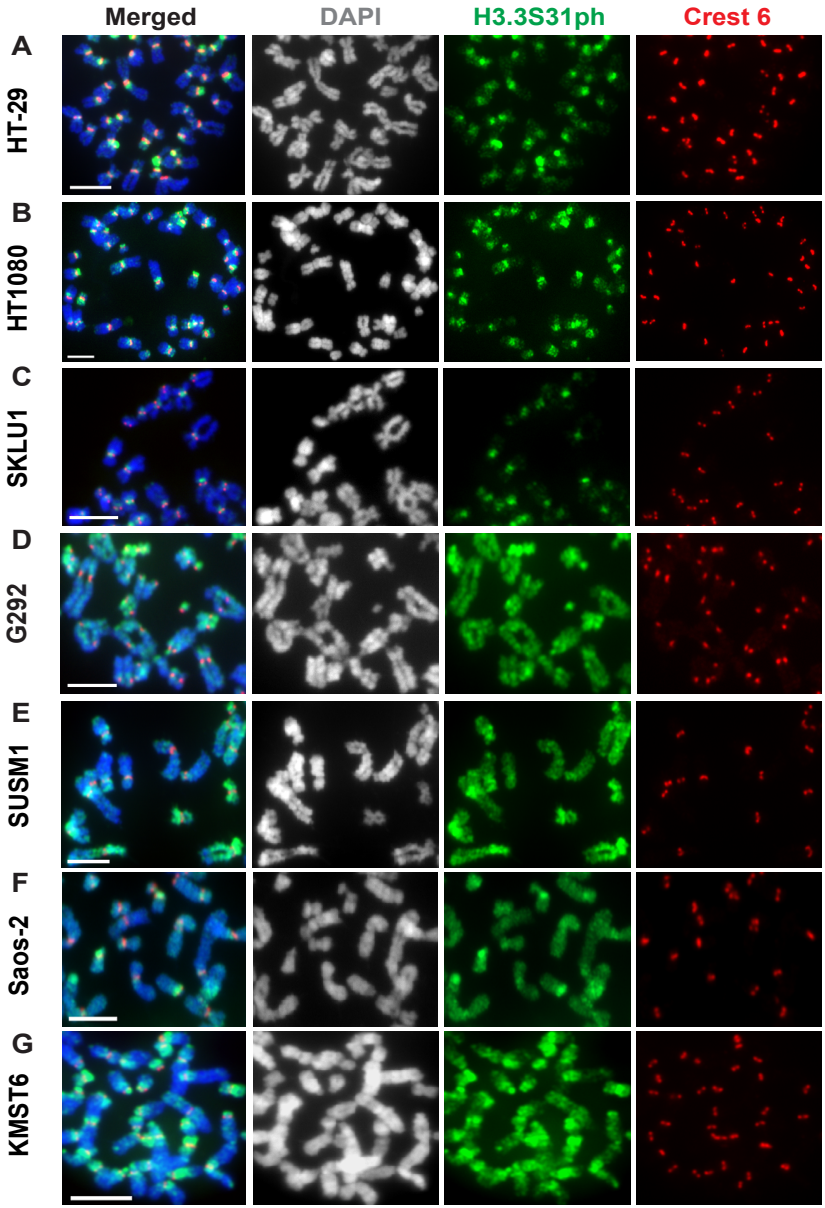
Merged
DAPI
H3.3S31ph
Crest 6
A
HT-29
B
HT1080
C
SKLU1
D
G292
E
SUSM1
F
Saos-2
G
KMST6

Figure S2

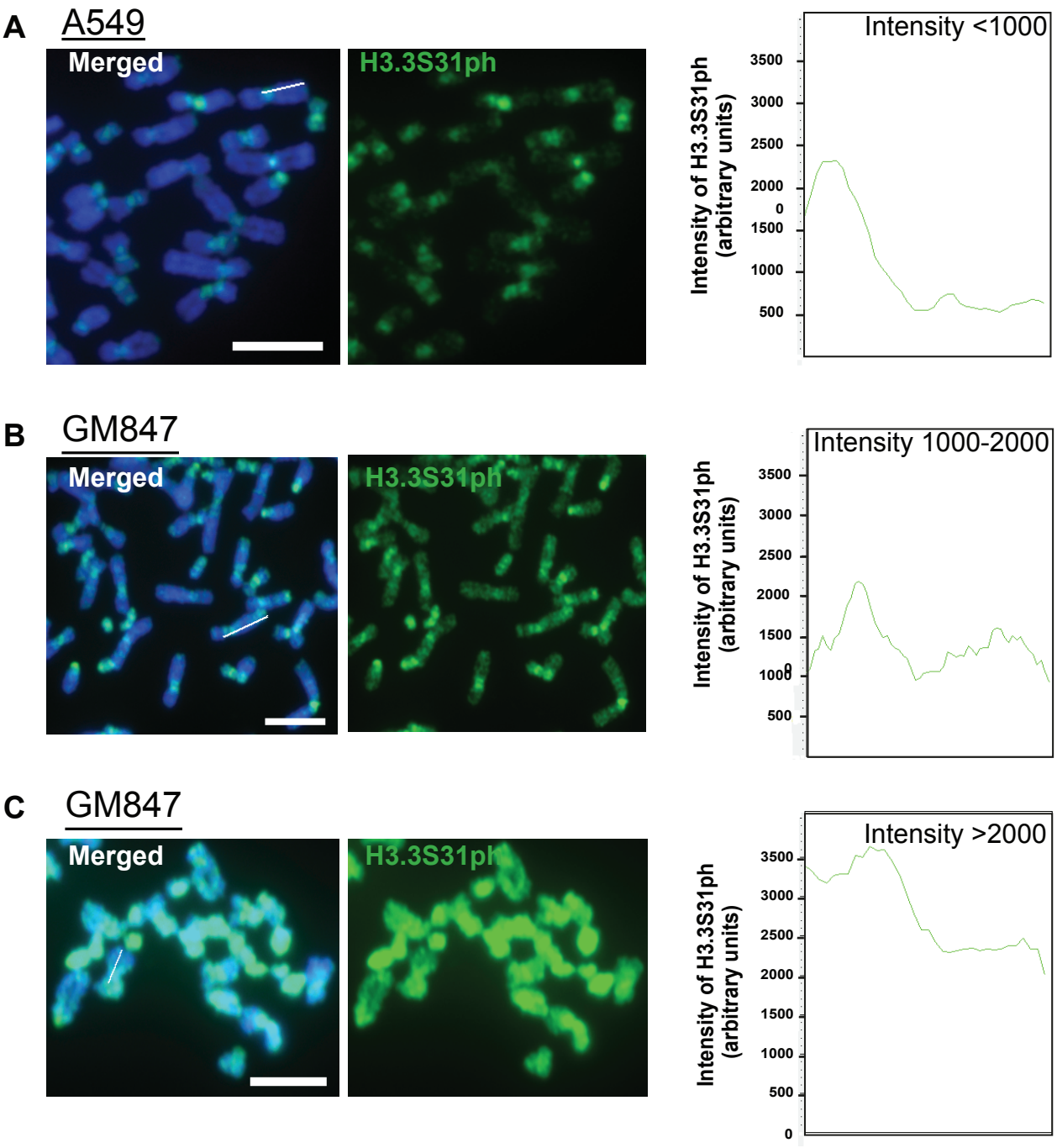

D

Intensity of H3.3S31ph staining on chromosome arms between non-ALT and ALT cells. The number of mitotic chromosome spreads is based on one experiment. A total of three independent experiments have been performed.

H3.3S31ph staining intensity on chromosome arms (arbitrary units)	A549	GM847
<1000	29 (91%)	9 (27%)
1000-2000	3 (9%)	17 (52%)
>2000	0 (0%)	7 (21%)
Total	32	33

Figure S3

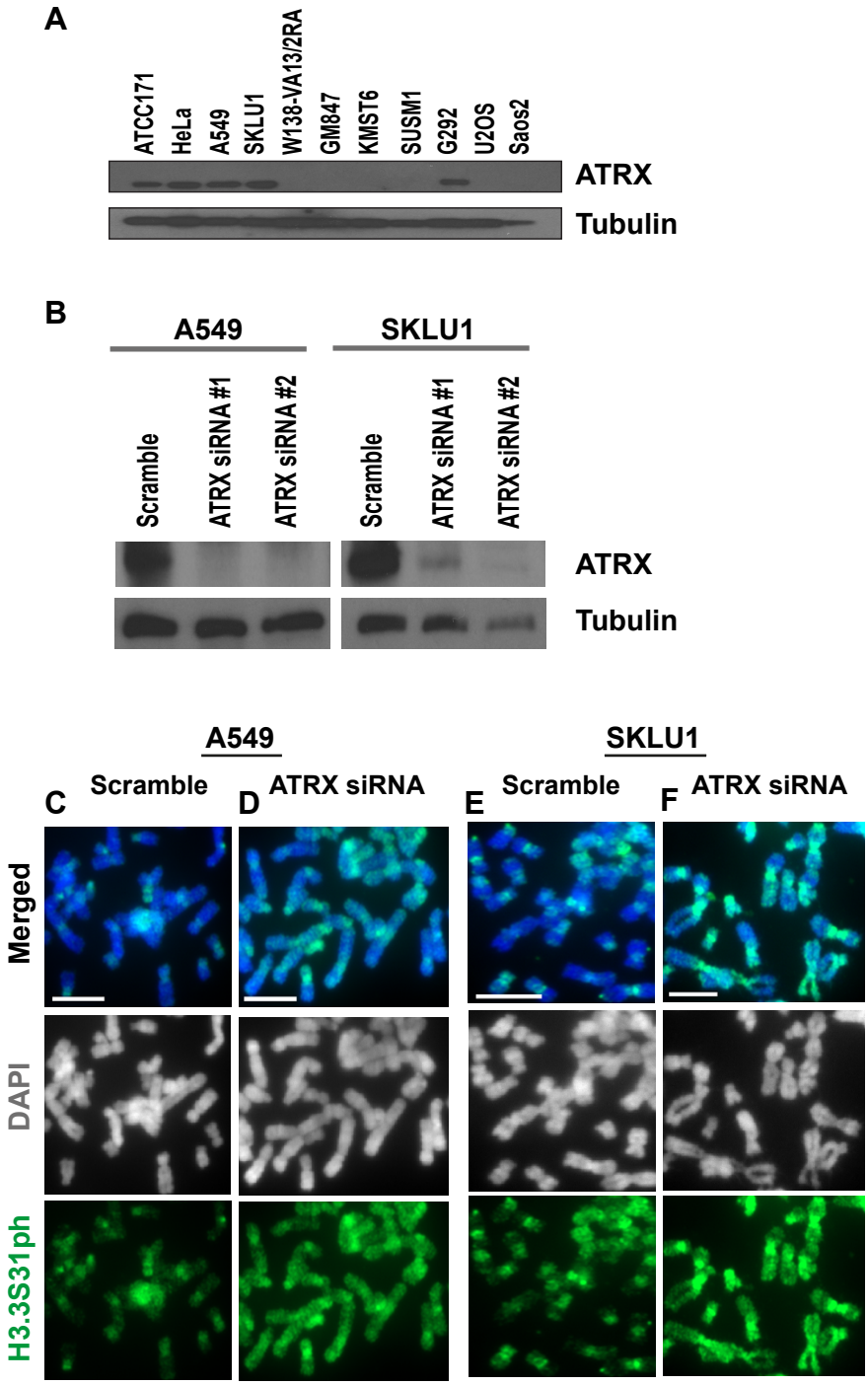
A
ATCC171
HeLa
A549
SKLU1
W138-VA13/2RA
GM847
KMST6
SUSM1
G292
U2OS
Saos2
ATRX
Tubulin
B
A549
SKLU1
Scramble
ATRX siRNA #1
ATRX siRNA #2
Scramble
ATRX siRNA #1
ATRX siRNA #2
ATRX
Tubulin
A549
SKLU1
C
Scramble
D
ATRX siRNA
E
Scramble
F
ATRX siRNA
Merged
DAPI
H3.3S31ph

Figure S4